A Control-Oriented Dynamic Model of Air Flow in a Single Duct HVAC System

Roshan RAISONI[1], Naren Srivaths RAMAN[1*], Prabir BAROOAH[1], Jeffrey D. MUNK[2], and Piljae IM[2]

[1]University of Florida, Department of Mechanical and Aerospace Engineering,
Gainesville, Florida, USA
roshanrai@ufl.edu, narensraman@ufl.edu, pbarooah@ufl.edu

[2]Oak Ridge National Laboratory,
Oak Ridge, Tennessee, USA
munkjd@ornl.gov, imp1@ornl.gov

[*]Corresponding author

ABSTRACT

A model of a variable air volume (VAV) system is developed that can predict air flow rates, fan pressure rise, and fan power consumption in response to changes in fan speed and damper positions. The system consists of a fan, ductwork, and a number of dampers, one in each VAV box. The model can be used for conducting simulation studies of how advanced control algorithms that seek to provide various services (energy efficiency, personalized comfort, and demand-side flexibility to the grid) may behave when deployed in a building with an existing climate control system, or to do model-based control computations for such services.

Comparison of the model's predictions with experimental data from a small commercial building is presented for the single-zone version of the model. The multi-zone model structure is described, but its validation is left for future work. Due to the strong non-linearities in the steady state relation between inputs and outputs, and due to the fast transient response observed in experiments, the dynamic model is constructed to be of Hammerstein type, with a linear dynamic system in series with a static nonlinear model.

1. INTRODUCTION

We present a simplified model of air flow for a variable air volume (VAV) system. The inputs to the model are the fan speed of the air handling unit (AHU) and the positions of the dampers at the VAV boxes. The outputs are air flow rates to the zones (through the VAV boxes), static pressure downstream of the fan, and fan power consumption.

The motivation for developing such a model comes from the recent interest in advanced control algorithms for heating, ventilation, and air conditioning (HVAC) systems with a view to provide high energy efficiency, personalized comfort, and demand-side flexibility to the grid. Current work in these directions have sought to obtain these services by keeping the existing climate control system in place and changing certain high-level setpoints. Since existing climate control systems use multiple hierarchies, changing a high-level setpoint may not provide desired performance. For instance, changing zone temperature setpoints to provide demand response service may produce a slower change in power consumption than desired (Goddard et al., 2014). This is because the zone level controllers have to react to the change in the setpoints first and reduce airflow rates. This will then changes the power demand experienced by the fan and the chiller, whose local controllers then will change their setpoints. The effect is therefore seen with some lag. Changing lower-level setpoints directly, such as changing the fan speed or static pressure setpoint to change power, will produce a faster change. But this has the risk of producing unintended consequences because of the complex interconnection

among various control hierarchies. For instance, reducing the fan speed will reduce airflow rate through the duct. The controllers at the VAV-boxes may then open up the dampers to increase their airflow rates to meet their local thermal and/or ventilation loads. The duct pressure will then change as a result, which will change the flow rates through the VAV boxes. Even if a steady-state is reached, the zones may not meet their ventilation or thermal constraints. We will present experimental evidence of such an unintended consequence in Section 1.1 of the paper.

A possible solution to these problems is to compute decisions for all the lower-level setpoints directly. This requires a model relating lower level control commands such as damper positions and fan speed to outputs such as airflow rate to zones, temperatures at various zones, and power consumptions of HVAC equipment, which can be used by optimizers to make appropriate decisions. If not for real-time control implementation, such a model is useful in simulation evaluation of control algorithms that seek to utilize existing control systems in place and vary intermediate-level setpoints.

There has been a large number of papers on modeling space temperatures of buildings, so we do not cover that topic here. Much less effort has been expended on modeling flow rates and duct pressures, mainly because model-free feedback control systems were sufficient so far, with in-situ tuning that is done during building commissioning. In this paper we focus on modeling airflow dynamics in a single-duct, multi-zone building. A zone is a space whose climate is controlled by a VAV box. The model we seek to develop predicts how the air flow to various zones (through their VAV boxes) change as the fan speed and VAV damper positions are changed. Because we envision the model to be used for real-time control computations, it needs to be a low order control oriented model. Experiments conducted in a small commercial building test facility is used to calibrate unknown parameters of the model, as well as evaluate prediction accuracy of the model.

Although there is a rich literature on modeling airflows in buildings (see (Axley, 2007; Feusel & Allard, 1990) and references therein), the number of works that model effect of damper positions on flow rates and duct pressure, such as (Haves et al., 1998), is quite limited. Relevant works include (Zaheer-Uddin & Zheng, 1994a, 1994b), which developed a dynamic model for a multi-zone VAV system. A weakness of this model is that the pressure rise across the fan was modeled as a function of the fan speed alone, whereas in practice this pressure rise depends on the air flow rate and thus the damper positions as well. In (Mei & Levermore, 2002), the authors developed and compared fan pressure models using artificial neural networks and polynomial curve fitting. Airflow rate was an input to the model whereas we are interested in modeling the effect of lower level actions such as fan speed and damper positions on the airflow. The reference (Haves et al., 1998) is also highly relevant to our work, as it developed a model capable of simulating airflow and pressure in response to damper positions and other low-level commands. The models were developed for use in HVACSIM+ and TRNSYS. Since the focus of (Haves et al., 1998) was modeling both airflow and thermal dynamics, along with the control loops, the resulting model is quite complex. A more recent work that sought to use the models developed in (Haves et al., 1998) for a demand response study found that TRNSYS had diffculty solving the large number of nonlinear equations embedded in those models (Blum & Norford, 2014). The reference (Blum & Norford, 2014) therefore performed simulations in Modelica using component models available in the Modelica Standard Library and the Modelica Library for Building Energy and Control Systems. In contrast, we seek to develop a low order model of the airflow and pressure dynamics that can be translated to any simulation platform.

Compared to the prior work, this paper makes the following contributions. One, we propose a model that relates zone air flows, fan pressure rise, and fan power (outputs) as a function of VAV box damper positions and AHU fan speed (inputs). These inputs can be independently varied in practice without creating feedback-induced interactions among other systems. The model can therefore be used to perform simulations of airflows for a diverse set of control applications, from energy efficiency improvements to demand response. We provide experimental validation of the model's prediction from data collected in a small commercial building (for the "single-zone" version). Two, we provide a Hammerstein model of the dynamics of fan power consumption, which is useful for designing control systems that use HVAC fans for fast grid-support applications such as contingency reserve and frequency regulation.

1.1 Example of Interactions Among Control Loops
Here we present results of an experiment that shows the unintended consequences that may result if low-level setpoints are varied without taking into account the interactions among various control loops. The model proposed here is motivated by the need to make decisions for lower levels loops in a consistent manner so that they do not interact in
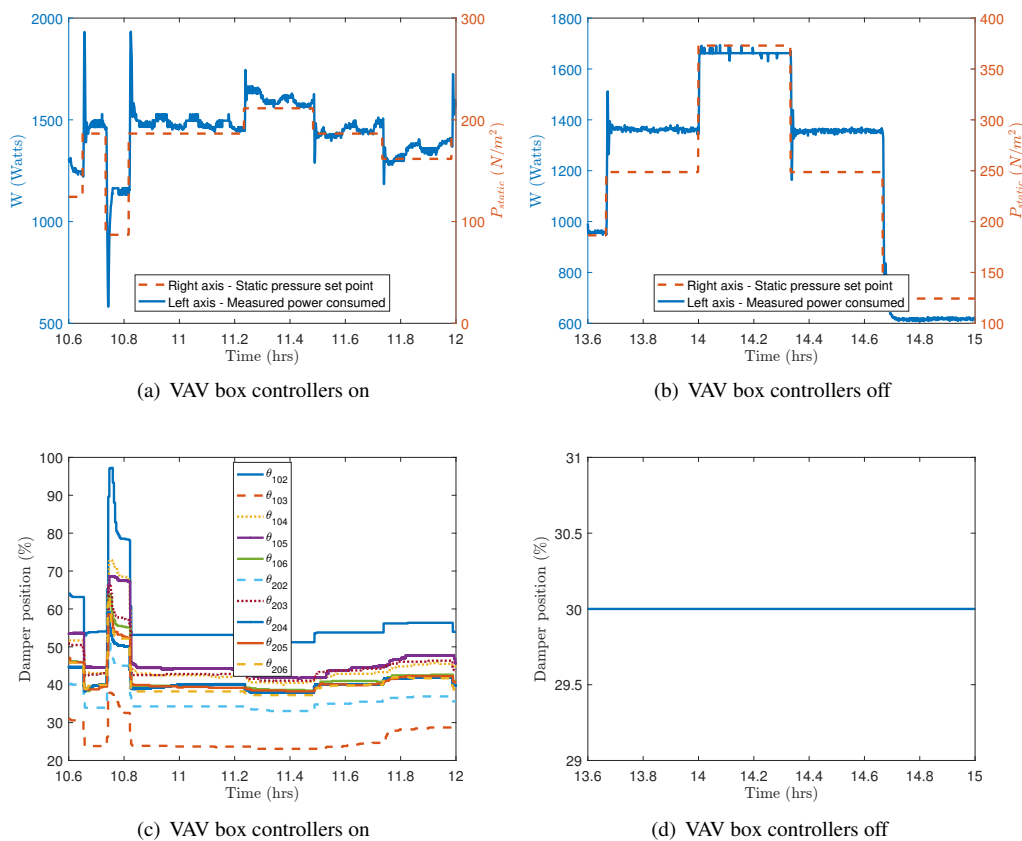
(a) VAV box controllers on

(b) VAV box controllers off

(c) VAV box controllers on

(d) VAV box controllers off

Figure 1: Fan power consumption variation in response to static pressure set point change.

a complex manner. The experiment was done on a small commercial building to see if varying fan static pressure setpoint of an air supply fan can change its power consumption in a predictable manner, when the rest of the climate control system is left untouched. The intended application was to provide demand response services to the grid through manipulation of power consumption.

The test was performed in a commercial building test facility that is described in more detail in Section 2.2. In this particular test, the static pressure set point was changed at intervals of 5 and 20 minutes. The resulting effect on consumption of fan power was recorded with a sampling period of 5 secs. Figure 1(a) shows the variation of output (fan power consumption) and input (static pressure set point) vs. time, under closed loop scenario. Meaning, the VAV boxes controllers were left untouched. The resulting actions of the VAV box dampers are shown in Figure 1(c).

The experiment was later repeated in an open-loop scenario, by turning off the VAV box damper controls and commanding all the dampers (there were 10 of them) to stay at a fixed position. Figure 1(b) shows the corresponding output (fan power consumption) and input (static pressure set point) vs. time.

It is clear from Figure 1(a) and Figure 1(b) that while the relationship between the fan static pressure setpoint and fan power consumption is quite consistent in the open-loop case, it is anything but in the closed loop case. The cause is visible from Figure 1(c): the complex feedback interaction between the VAV box damper control and duct pressure-flow dynamics. Thus, varying fan static pressure set point while leaving the zone-level controllers untouched will not lead to a predictable power consumption variation. These observations are consistent with those in (Blum & Norford, 2014).

A model of the kind proposed here can be used to compute appropriate commands for the damper positions so that together with the pressure/flow rate setpoints, a predictable power consumption results.

2. SINGLE-ZONE STEADY STATE MODEL

The model we seek to develop is a low-order dynamic model for a single duct VAV HVAC system as shown in Figure 2(a). The inputs to the model are fan speed N_f and damper positions θ_i $i = 1, \ldots, n$, where n is the number of VAV boxes. Both fan speed and damper positions are typically expressed as percentage (of a rated value). The main outputs of interest are supply air flow rate (Q) through the AHU, air flow rates through the VAV boxes (Q_i, $i = 1, \ldots, n$), pressure rise across the fan (P_{fan}), and the electrical power consumed by the fan (W).

(a) Single-zone model.   (b) Pressure variation in the single-zone system.
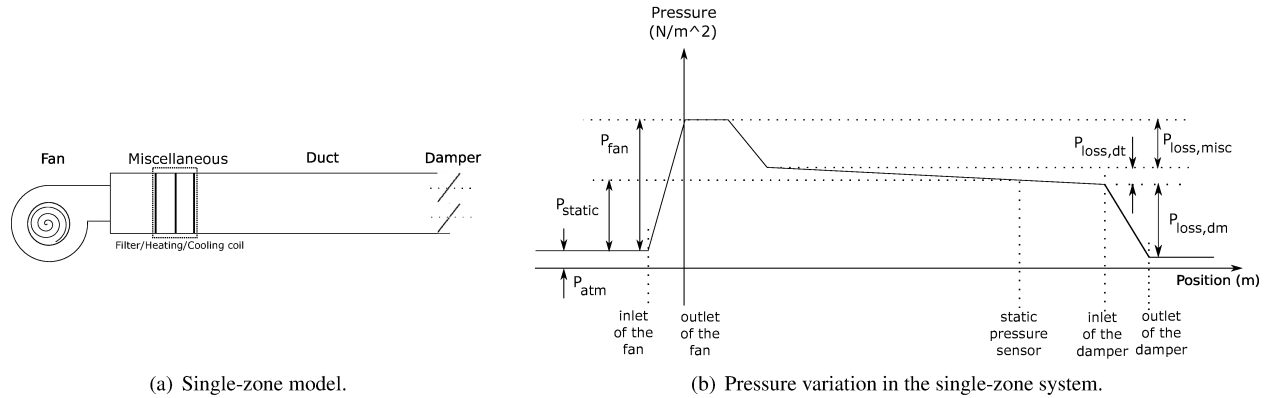
Figure 2: Single-zone system layout and various pressure terms.

We first describe the model for a simple configuration, in which there is only one zone, i.e. $n = 1$. It will serve as a stepping stone for extension to multiple zones. We focus first on the steady-state relationships, ignoring dynamics.

2.1 Model Description

Since there is only one zone, there are only two independent variables θ and N_f. The outputs of interest are fan static pressure rise P_{fan}, the flow rate through the system Q, and power W. The total pressure change across the entire system consists of pressure rise across the fan, pressure loss along the duct, pressure loss across the damper, and a miscellaneous pressure loss that occurs due to filters and cooling/heating coils. Figure 2(b) shows the various pressure changes in the system. For a given fan speed and air flow rate, the fan pressure rise is given by

$$P_{fan} = a_{f_0} + a_{f_1} N_f Q + a_{f_2} Q^2, \tag{1}$$

where a_{f_i}'s are constants that depend on, geometry of the fan and velocity of air at inlet of the fan. A detailed derivation of this model is provided in Appendix A.

The pressure loss in a duct is given by the Darcy equation (ASHRAE, 2013) as

$$P_{loss,dt} = 1000 f L \rho V_{dt}^2 / (2D_h),$$

where ρ is the density of air, L is the duct length, V_{dt} is velocity of air in the duct, f is the friction factor, and $D_h = 4A_{dt}/P$ is the hydraulic diameter, where P is perimeter of cross-section of the duct and A_{dt} is area of the duct. The friction factor f (Jorgensen, 1999) is given as $f = 0.25/(\log(\frac{\varepsilon/D_h}{3.7} + \frac{5.74}{Re^{0.9}}))^2$, where ε is the absolute roughness of the duct material and $Re = \frac{\rho V_{dt} D_h}{\mu}$ is the Reynolds number, where μ is the absolute viscosity of air. Note that f is a function of Q and will be written as $f(Q)$, since the Reynolds number Re is a function of V_{dt}, and $V_{dt} = Q/A_{dt}$. Combining all of this, $P_{loss,dt}$ can be expressed as

$$P_{loss,dt} = \frac{1000 L \rho}{2 D_h A_{dt}^2} f(Q) Q^2. \tag{2}$$

The pressure loss across the damper is modeled as (Zaheer-Uddin & Zheng, 1994b)

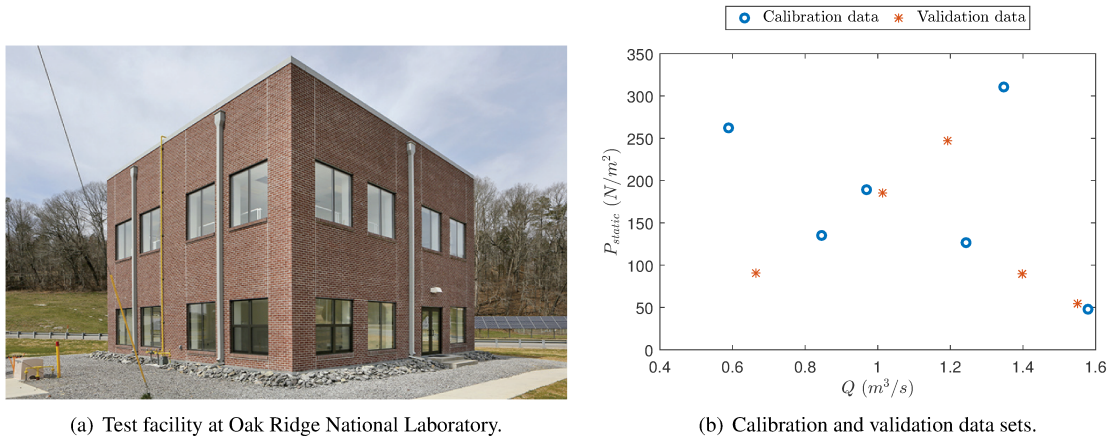$$P_{loss,dm} = \{a_{d_0} exp(a_{d_1} \theta)\} \rho V_{dm}^2 / 2, \tag{3}$$

(a) Test facility at Oak Ridge National Laboratory.

(b) Calibration and validation data sets.

Figure 3: Test facility and experimental data sets.

where θ is the damper position, V_{dm} is velocity of air through open area of the damper, and a_{d_i}'s are constants that depend on the damper. More specifically, θ is a number between $[0, 100]$, where $\theta = 0$ indicates the damper is fully closed, and $\theta = 100$ indicates the damper is fully open. Since $V_{dm} = Q/A_{dm}^{(\theta)}$, where $A_{dm}^{(\theta)}$ is the area of damper that is available for the air to flow for a particular θ. If $A_{dm}^{(n)}$ is the nominal area of the damper i.e. area which is available for the air to flow for a fully open damper, then $A_{dm}^{(\theta)} = A_{dm}^{(n)}\left(1 - \cos\left(\frac{\pi}{2}\theta\right)\right)$. Substituting these expressions for V_{dm} and $A_{dm}^{(\theta)}$ in (3), we get

$$P_{loss,dm} = \{a_{d_0} exp(a_{d_1}\theta)\} \frac{\rho}{2\left(A_{dm}^{(\theta)}\right)^2} Q^2. \tag{4}$$

The pressure loss due to filters and heating/cooling coils is modeled as a quadratic function of the flow rate

$$P_{loss,misc} = a_{m_0} + a_{m_1}Q + a_{m_2}Q^2, \tag{5}$$

where a_{m_i}'s are constants dependent on the properties of filters and heating/cooling coils used. By combining (1), (2), (4), and (5), we obtain, $0 = P_{fan} - P_{loss,misc} - P_{loss,dt} - P_{loss,dm}$. Thus,

$$0 = \left[a_{f_0} + a_{f_1}N_f Q + a_{f_2}Q^2\right] - \left[a_{m_0} + a_{m_1}Q + a_{m_2}Q^2\right] - \left[\frac{1000L\rho}{2D_h A_{dt}^2}f(Q)Q^2\right] - \left[\{a_{d_0}exp(a_{d_1}\theta)\}\frac{\rho}{2(A_{dm}^{(\theta)})^2}Q^2\right]. \tag{6}$$

The right hand side is a function of θ, N_f and Q. For a given N_f and θ, we can find Q by solving (6). For future convenience we express this solution as

$$Q = g(\theta, N_f). \tag{7}$$

Once Q is determined, all the pressure rise/drops can be computed from (1), (2), (4), and (5). Furthermore, the electrical power consumed by the fan motor is given as (Jorgensen, 1999)

$$W = P_{fan}Q/\eta, \tag{8}$$

where η is the combined efficiency of the motor and fan, which can also be computed once Q is known.

2.2 Model Calibration and Validation from Experimental Data

The model ((1), (4), and (5)) has 8 unknown parameters: a_{f_0}, a_{f_1}, a_{f_2}, a_{d_0}, a_{d_1}, a_{m_0}, a_{m_1}, and a_{m_2}. These must be determined from measurements and/or manufacturer-provided data since they vary from one building/equipment to another. A variety of tests were done at a test facility located in the Oak Ridge National Laboratory (ORNL) campus, Tennessee. The test facility is shown in Figure 3(a). It is a two story building, with a floor area of ~ 150 m^2, with ten rooms, each with its own VAV box. To mimic a single-zone system, all 10 VAV dampers were operated in unison. The following tests were performed:

- Test 1: The fan speed was kept constant at 75% and readings were obtained for various damper positions.
- Test 2: The damper positions were kept constant at 30% and readings were obtained for various fan speeds.

At each test condition, raw data was collected at a high sampling rate, and steady state data was obtained by waiting for the response to settle down. The test data was divided into two sets for calibration and validation as shown in Figure 3(b).
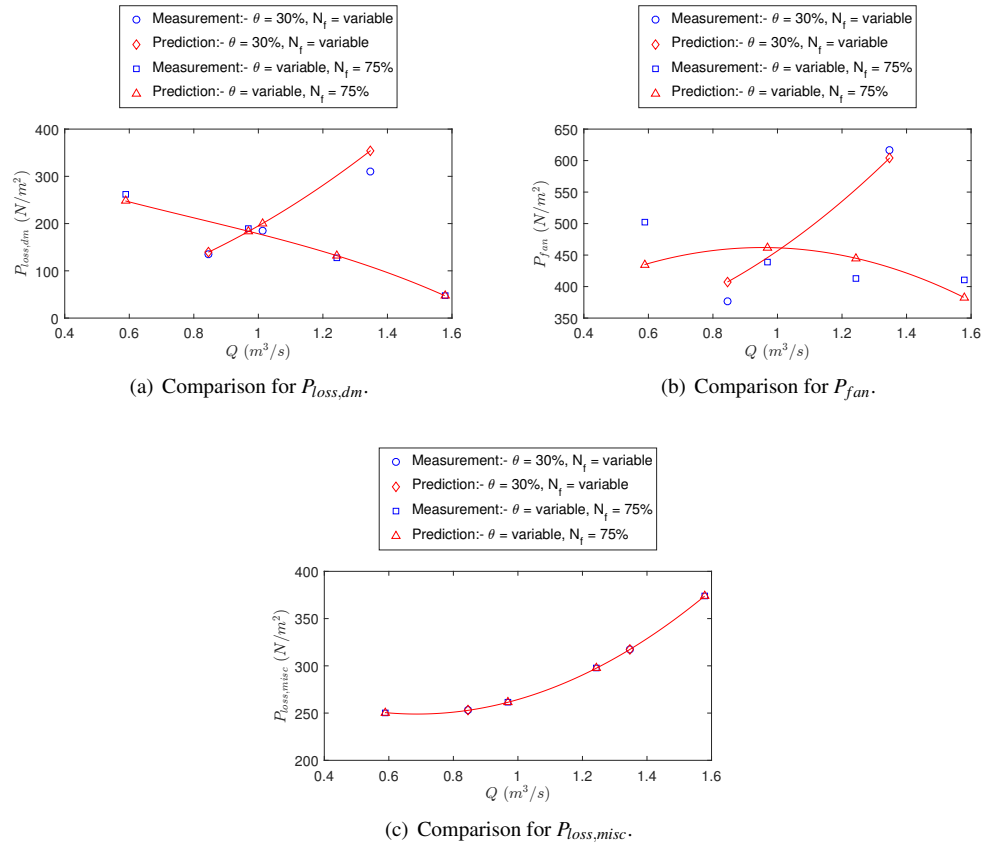

(a) Comparison for $P_{loss,dm}$.

(b) Comparison for P_{fan}.

(c) Comparison for $P_{loss,misc}$.

Figure 4: Calibration data set: Measurements and Predictions.

2.2.1 Model calibration: To fit the damper parameters (a_{d_0} and a_{d_1} in (3)), we need $P_{loss,dm}$ readings at various damper positions and air flow rates. The static pressure sensor is placed $2/3rd$ down the duct as shown in Figure 2(b). Assuming the duct pressure losses to be negligible compared to the damper pressure losses, $P_{loss,dm} \approx P_{static}$. With this assumption, rearranging and taking log on both sides of (4) we have

$$\log a_{d_0} + a_{d_1}\theta = \log\left(2P_{loss,dm}(A_{dm}^{(\theta)})^2/(\rho Q^2)\right). \tag{9}$$

Since (9) is linear in $\log a_{d_0}$ and a_{d_1}, we use least squares regression to estimate the two parameters. Figure 4(a) compares the measured $P_{loss,dm}$ to the prediction from the estimated parameters for a given air flow rate and damper position.

To fit the fan parameters (a_{f_0}, a_{f_1}, and a_{f_2} in (1)), we need P_{fan} readings at various fan speeds and air flow rates. P_{fan} is the pressure rise across the inlet and outlet of the fan. Assuming a constant efficiency, P_{fan} can be computed by rearranging (8) as $P_{fan} = \eta W/Q$. Since (1) is linear in a_{f_0}, a_{f_1}, and a_{f_2}, we use least squares regression to estimate these three parameters. Figure 4(b) compares the measured P_{fan} to the prediction from the estimated parameters for a given air flow rate and fan speed.

To fit the miscellaneous pressure loss parameters (a_{m_0}, a_{m_1}, and a_{m_2}) in (5), we need P_{misc} readings at various air flow rates. Assuming duct pressure losses to be negligible, rearranging (6) we have $P_{loss,misc} = P_{fan} - P_{loss,dm}$. Since (5)

is linear in a_{m_0}, a_{m_1}, and a_{m_2} we use least squares regression to estimate these parameters. Figure 4(c) compares the measured $P_{loss,misc}$ to the prediction from the estimated parameters for a given air flow rate.

2.2.2 Model validation: Once a_{f_0}, a_{f_1}, a_{f_2}, a_{d_0}, a_{d_1}, a_{m_0}, a_{m_1}, and a_{m_2} are estimated, the model ((7), (1) and (8)) is used to predict Q, P_{fan}, and W for an input fan speed and damper position. The data set shown in Figure 3(b) is used for model validation. Figures 5(a) - 5(c) show a comparison of the measured data and predictions from our model. The predictions show the following root-mean-square errors: Q (0.065 m^3/s), P_{fan} (13 N/m^2) and W (36.9 Watts).

(a) Comparison for W ($\theta = 30\%$ and N_f is varying).

(b) Comparison for W ($N_f = 75\%$ and θ is varying).
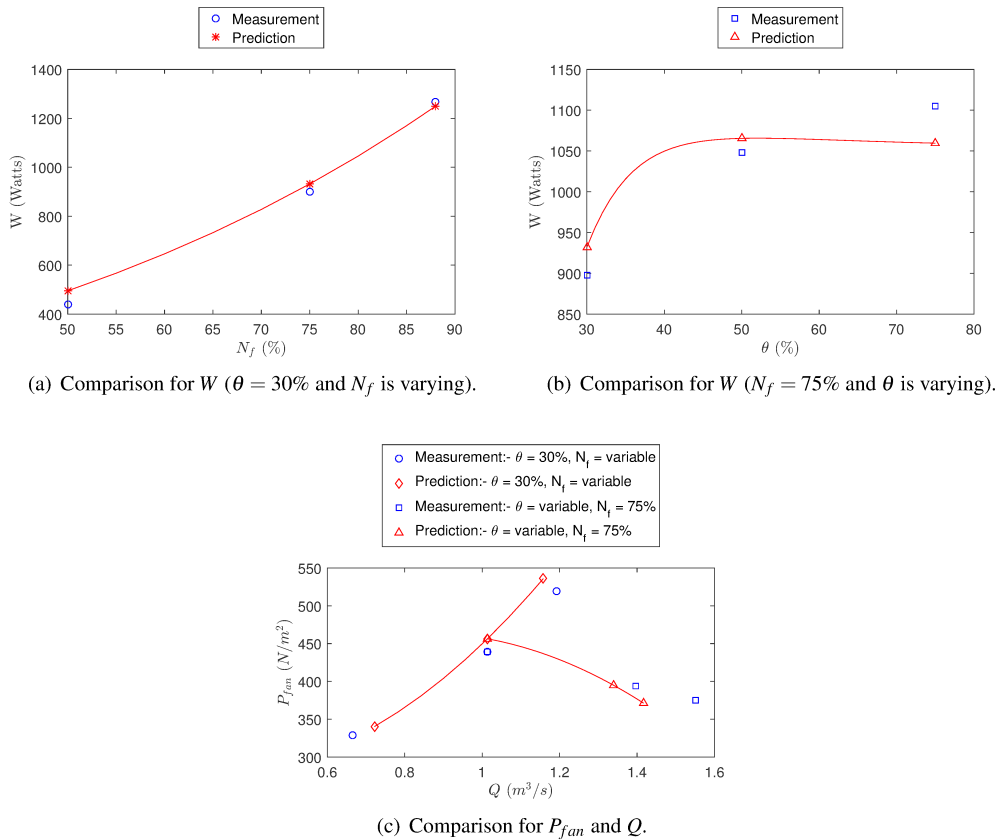

(c) Comparison for P_{fan} and Q.

Figure 5: Validation data set: Measurements and Predictions.

3. SINGLE-ZONE DYNAMIC MODEL

The results from step response tests as described in Section 2.2 are shown in Figure 7. The Hammerstein form (Ljung, 1999) was used to introduce dynamics in our model as seen in Figure 6, where $H(.)$ is a vector function with input as $[\theta; N_f]$ and output as $Y = [Q; P_{fan}; W]$ obtained from our model ((1), (7), and (8)) and the time constant τ, was computed to be 26, 11, and 6 secs for Q, P_{fan}, and W respectively.
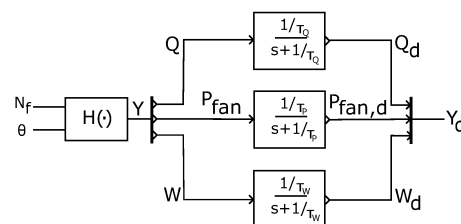

Figure 6: Hammerstein form for dynamics of the model.

(a) Comparison for Q ($\theta = 30\%$ and N_f is varying).

(b) Comparison for P_{static} ($\theta = 30\%$ and N_f is varying).

(c) Comparison for W ($\theta = 30\%$ and N_f is varying).
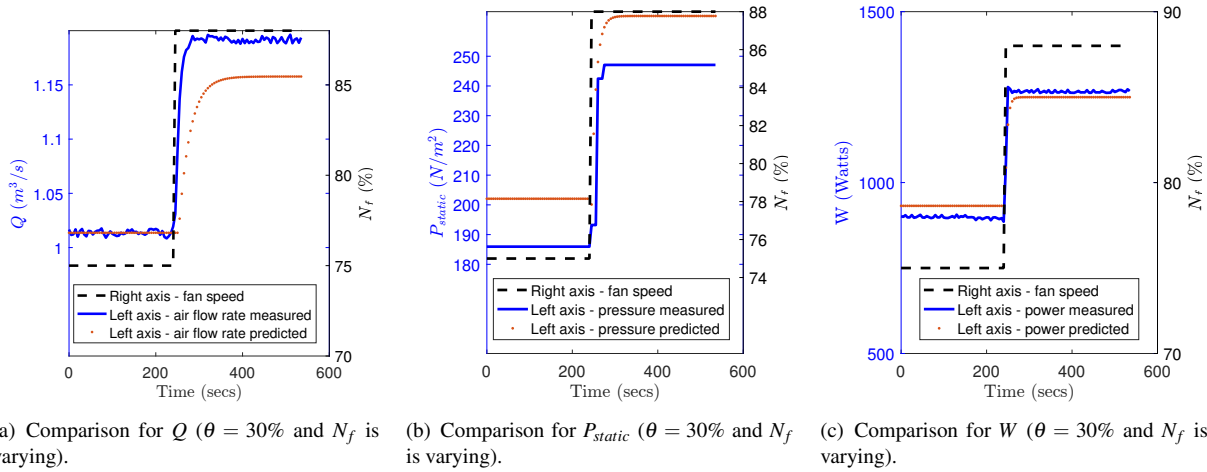
Figure 7: Dynamic model: Measurements and Predictions.

4. MULTI-ZONE MODEL

Here we consider the case with *n* VAV boxes. We consider a tree graph layout of the duct system which is found in most buildings. Without loss of generality consider the layout shown in Figure 8. Every end branch has a damper which allows air to flow into each zone. In Figure 8 there are 9 nodes (0,1,2,...) which have different pressures. Air flows from node 0 before the fan to node 0 after each damper along a specific path. The pressure rise and pressure drops along each path consists of the same kinds of terms that were described in the single-zone model. For example, consider the path P_{c_2} across damper 'c2' from node 0 before the fan to node 0 after the damper, $P_{c_2} = \left[\{0,1\}, \{1,2\}, \{2,4\}, \{4,5\}, \{5,0\} \right]$. This path is a combination of fan, filter and heating/cooling coils, duct, and damper. By pressure balance, in steady state we have

$$0 = P_{fan} - P_{loss,misc} - P_{loss,dt\{2,4\}} - P_{loss,dt\{4,5\}} - P_{loss,dm,c2}$$

$$= \left[a_{f_0} + a_{f_1} N_f Q + a_{f_2} Q^2 \right] - \left[a_{m_0} + a_{m_1} Q + a_{m_2} Q^2 \right] - \left[\frac{1000 L \rho}{2 D_h A_{dt}^2} f(Q_c) Q_c^2 \right] - \left[\frac{1000 L \rho}{2 D_h A_{dt}^2} f(Q_c - Q_{c1})(Q_c - Q_{c_1})^2 \right]$$

$$- \left\{ a_{d_0} exp(a_{d_1} \theta_{b_2}) \right\} \frac{\rho}{2(A_{dm,\theta_{b_2}})^2} Q_{c_2}^2. \tag{10}$$

where the second equation is obtained by using (1), (2), (4), and (5). For 6 dampers, we have 6 such equations, and 6 unknowns: Q_{a_1}, Q_{a_2}, Q_{b_1}, Q_{c_1}, Q_{c_2} and Q_{c_3}. These 6 equations can be solved to obtain the value of $\bar{Q} = [Q_{a_1}, Q_{a_2}, Q_{a_3}, Q_{b_1}, Q_{c_1}, Q_{c_2}]^T \in \mathbb{R}^6$ for a given $\bar{\theta} = [\theta_1, \ldots, \theta_6]^T \in \mathbb{R}^6$ and N_f. The solution can be represented as,

$$\bar{Q} = \bar{g}(\bar{\theta}, N_f) \tag{11}$$

which is the model for the 6-zone system. For a general *n*-zone system the same process applies. We believe the transient response can be captured by using a Hammerstein structure, as was done in the single-zone model. We are currently in the process of obtaining experimental data for calibrating the unknown parameters in the multi-zone model, testing its predictions, and determining its transient response. The same test facility will be used as it has 10 zones.

5. CONCLUSION

A model that can predict the flow rates and various pressure rise/drops, along with the fan power consumption was presented. Validation with experimental data was presented for the single-zone case. It was found that the model predictions are accurate except for very small values of the damper positions. Validation for the multi-zone case is ongoing and will be reported elsewhere.
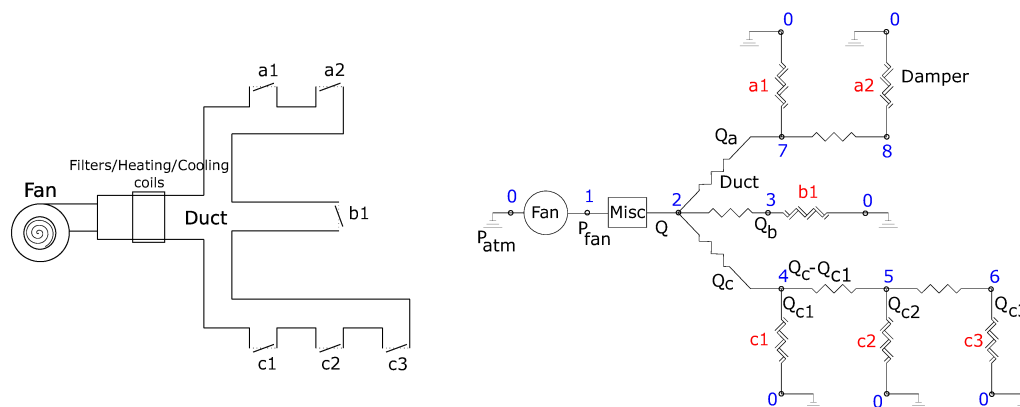
Figure 8: Multi-zone model

There are several additional avenues for future work. Fan efficiency was assumed constant. Modeling it as a function of flow rate and fan speed is likely to increase prediction accuracy. The proposed model has several unknown parameters that vary from one air distribution system to another. In this work we fitted those parameters from data obtained from specially designed experiments. In the future we will explore ways to fit them from normal operation data so that special experiments are not needed, or ways to minimize the number of special experiments needed to fit them.

REFERENCES

ASHRAE, F. (2013). Fundamentals handbook. *IP Edition*, 21.6.

Axley, J. (2007). Multizone airflow modeling in buildings: History and theory. *HVAC&R Research*, *13*(6), 907–928.

Blum, D. H., & Norford, L. K. (2014). Dynamic simulation and analysis of ancillary service demand response strategies for variable air volume hvac systems. *HVAC&R Research*, *20*(8), 908–921.

Feusel, H. E., & Allard, F. (1990). *Fundamentals of the multizone air flow model-comis*. Oscar Faber.

Goddard, G., Klose, J., & Backhaus, S. (2014, July). Model development and identification for fast demand response in commercial hvac systems. *IEEE Transactions on Smart Grid*, *5*(4), 2084-2092. doi: 10.1109/TSG.2014 .2312430

Haves, P., Norford, L. K., & DeSimone, M. (1998). A standard simulation test bed for the evaluation of control algorithms and strategies. *ASHRAE transactions*, *104*, 460.

Jorgensen, R. (1999). *Fan engineering: An engineer's handbook on fans and their applications; howden buffalo.* Inc.

Ljung, L. (1999). *System identification: Theory for the user* (2nd ed.). Prentice Hall.

Mei, L., & Levermore, G. (2002). Simulation and validation of a vav system with an ann fan model and a non-linear vav box model. *Building and Environment*, *37*(3), 277–284.

Zaheer-Uddin, M., & Zheng, G. (1994a). A dynamic model of a multizone vav system for control analysis. *Transactions-American Society of Heating Refrigerating and Air Conditioning Engineers*, *100*, 219–219.

Zaheer-Uddin, M., & Zheng, G. (1994b). A vav system model for simulation of energy management control functions: off normal operation and duty cycling. *Energy conversion and management*, *35*(11), 917–931.

ACKNOWLEDGMENT

APPENDIX A. FAN MODEL

The external torque, T acting on the fan that provides energy to air can be given as, $T = \dot{m}(r_2 v_{2_t} - r_1 v_{1_t})$ where, $\dot{m}$ is the mass flow rate of air, r is the fan blade radius and v is the air velocity. Subscripts, 1, 2 denote the inlet and exit of air to and from the fan and t denotes the tangential velocity of air. If fan is rotating with an angular velocity of ω, the

mechanical power required to maintain the air flow will be,

$$W_{mech} = T\omega \quad \Rightarrow \quad W_{mech} = \dot{m}(r_2 v_{2_t} - r_1 v_{1_t})\omega \quad \Rightarrow \quad W_{mech} = \dot{m}(u_2 v_{2_t} - u_1 v_{1_t})$$

where, u is the blade tip velocity. The pressure head required to maintain this air flow is given by,

$$P_{total} = W_{mech}/\dot{m}g \quad \Rightarrow \quad P_{total} = (u_2 v_{2_t} - u_1 v_{1_t})/g$$

The radial component of fluid velocity at exit of the impeller determines the air flow rate, Q.

$$Q = 2\pi r_2 b_2 v_{2_r} \quad \Rightarrow \quad v_{2_r} = Q/(2\pi r_2 b_2) \tag{12}$$

where, b is the width of the blade and subscript r denotes radial component. At the inlet of a centrifugal fan, the air flow velocity will be radial. So its tangential component $v_{1_t} = 0$. Thus, the pressure head developed by the fan can be simplified as,

$$P_{total} = u_2 v_{2_t}/g \tag{13}$$

The blade angle β of a fan is obtained from blade geometry of the fan and can be represented as,

$$\cot\beta_2 = (u_2 - v_{2_t})/v_{2_r} \quad \Rightarrow \quad v_{2_t} = u_2 - \cot\beta_2 v_{2_r} \tag{14}$$

Substituting the value of v_{2_r} and v_{2_t} from equations (12) and (14) into equation (13), pressure head developed by the fan is expressed as,

$$P_{total} = \frac{1}{g}\left(u_2^2 - \frac{\cot\beta_2}{2\pi r_2 b_2}u_2 Q\right) \tag{15}$$

Also, v_2 can be broken down as,

$$v_2^2 = v_{2_t}^2 + v_{2_r}^2 \quad \Rightarrow \quad v_2^2 = \left(u_2 - \cot\beta_2 v_{2_r}\right)^2 + \left(Q/(2\pi r_2 b_2)\right)^2 \tag{16}$$

The total pressure head developed by the fan can also be written as,

$$P_{total} = P_{dynamic} + P_{fan} \quad \Rightarrow \quad P_{fan} = P_{total} - P_{dynamic} \tag{17}$$

where, P_{fan} and $P_{dynamic}$ are the static and dynamic pressure heads across the fan. $P_{dynamic}$ can also be expressed as,

$$P_{dynamic} = (v_2^2 - v_1^2)/g \tag{18}$$

Substituting the value of $P_{dynamic}$ and v_2^2 from equation (18) and (16) in (17), we can express P_{fan} as,

$$P_{fan} = u_2^2 - \frac{\cot\beta_2}{2\pi r_2 b_2}u_2 Q - v_2^2 + v_1^2$$

$$\Rightarrow P_{fan} = u_2^2 - \frac{\cot\beta_2}{2\pi r_2 b_2}u_2 Q - u_2^2 + 2u_2\cot\beta_2\frac{Q}{2\pi r_2 b_2} - \cot^2\beta_2\left(\frac{Q}{2\pi r_2 b_2}\right)^2 - \left(\frac{Q}{2\pi r_2 b_2}\right)^2 + v_1^2$$

$$\Rightarrow P_{fan} = \frac{\cot\beta_2}{2\pi r_2 b_2}u_2 Q - \cot^2\beta_2\left(\frac{Q}{2\pi r_2 b_2}\right)^2 - \left(\frac{Q}{2\pi r_2 b_2}\right)^2 + v_1^2$$

$$\Rightarrow P_{fan} = \frac{\cot\beta_2}{2\pi b_2}\omega Q + \left(\frac{-\cot^2\beta_2 - 1}{2\pi r_2 b_2}\right)Q^2 + v_1^2 \tag{19}$$

If ω_n is the maximum angular velocity of the fan, and $N_f = 100\frac{\omega}{\omega_n}$ is the fan percent we can rewrite equation (19) as,

$$P_{fan} = \frac{\cot\beta_2\omega_n}{200\pi b_2}N_f Q + \left(\frac{-\cot^2\beta_2 - 1}{2\pi r_2 b_2}\right)Q^2 + v_1^2 \quad \Rightarrow \quad P_{fan} = a_{f_0} + a_{f_1}N_f Q + a_{f_2}Q^2 \tag{20}$$